

Two Novel Acentric Borate Fluorides:  $M_3B_6O_{11}F_2$  ( $M = Sr, Ba$ )

Colin D. McMillen, Jared T. Stritzinger, and Joseph W. Kolis\*

Department of Chemistry and Center for Optical Materials Science and Engineering Technologies (COMSET), Clemson University, Clemson, South Carolina 29634, United States

## Supporting Information

**ABSTRACT:** Two novel, noncentrosymmetric borate fluorides,  $Sr_3B_6O_{11}F_2$  and  $Ba_3B_6O_{11}F_2$ , have been synthesized hydrothermally and their structures determined. The compounds are isostructural, crystallizing in space group  $P2_1$ , having lattice parameters of  $a = 6.4093$  (13) Å,  $b = 8.2898$  (17) Å,  $c = 9.3656$  (19) Å, and  $\beta = 101.51$  (3)° for  $Sr_3B_6O_{11}F_2$  and  $a = 6.5572$  (13) Å,  $b = 8.5107$  (17) Å,  $c = 9.6726$  (19) Å, and  $\beta = 101.21$  (3)° for  $Ba_3B_6O_{11}F_2$ . The structure consists of a complex triple-ring borate framework having aligned triangular  $[BO_3]$  groups that impart polarity. Fluorine atoms are bound only to the alkaline-earth metals and are not part of the borate framework, resulting in a vastly different structure from those of the hydrated borates  $Sr_3B_6O_{11}(OH)_2$  and  $Ba_3B_6O_{11}(OH)_2$  with similar formulas. The title compounds are transparent to nearly 200 nm, making them potentially useful for deep-ultraviolet nonlinear-optical applications.

The development of the structural chemistry of metal borates is of considerable interest because of their potential application in deep-ultraviolet (UV) nonlinear-optical (NLO) applications, especially for very short-wavelength (<266 nm) solid-state lasers.<sup>1</sup> Metal borates have a vast and interesting structural chemistry with several unique characteristics. They often have band edges well into the deep-UV, often below 200 nm.<sup>2,3</sup> Also, they crystallize in noncentrosymmetric (NCS) space groups at a much higher rate than inorganic solids in general (~35% for borates versus 11% for all inorganic solids).<sup>4</sup> In recent years, we demonstrated that a wide variety of novel alkali and alkaline-earth (AE) metal borates could be grown using hydrothermal methods.<sup>5–7</sup> In particular, we investigated the chemistry of strontium and barium borates because of the technological importance of commercial materials like  $\beta$ - $BaB_2O_4$ . We find an extensive descriptive chemistry of strontium and barium borates in hydrothermal fluids.<sup>8,9</sup> Although many of these are acentric and some of these show considerable promise, a significant limitation is the tendency to form solids containing  $OH^-$  groups bound to the boron atoms.<sup>9</sup> This is a problem because those crystals tend to exhibit a high thermo-optical coefficient, making them less useful for laser applications. Thus, we are seeking a hydrothermal route to NCS borates that do not contain  $OH^-$  groups.

In this paper, we report a route to new NCS borate crystals. By introducing fluoride into the starting materials and using it as a mineralizer, we can generate new NCS fluoroborates or borate fluorides. The fluoride ions can formally replace  $OH^-$  groups in the structures and do not suffer the same

shortcomings as the hydrated compounds. These fluoride-containing compounds have wide band gaps and are stable toward hydrolysis.<sup>10,11</sup> They also are thermally stable with high optical damage thresholds. In this paper, we report on the first in a potentially large series of new NCS metal borate fluoride single crystals prepared using hydrothermal methods. The title compounds  $M_3B_6O_{11}F_2$  have formulas similar to our recently isolated  $M_3B_6O_{11}(OH)_2$  class of compounds (see the accompanying paper in this journal). However, the title compounds have different structures that are also NCS, making them very promising for deep-UV NLO applications. Given the extensive number of hydrated metal borates that can be isolated from hydrothermal fluids, we feel that the formal substitution of  $OH^-$  with  $F^-$  in this class of compounds could provide a route to an enormous number of important NLO and laser crystals.

Crystals of the title compounds were synthesized by a two-step process. Polycrystalline borate feedstock precursors were first synthesized through solid-state reactions. Powders of  $MF_2$  (99%), 6 equiv of  $H_3BO_3$  (99.5%), and 4 equiv of  $NH_4F$  (98%) were mixed thoroughly, ground, and heated in a platinum crucible at 800 °C for 24 h. The resulting polycrystalline powder was then used as a feedstock (0.15 g) in hydrothermal reactions in welded silver ampules with 0.4 mL of 2 M KF mineralizer for  $Sr_3B_6O_{11}F_2$  and 3 M  $KHF_2$  for  $Ba_3B_6O_{11}F_2$  at 540 °C for 7 days. The reaction products were characterized by powder and single-crystal X-ray diffraction (XRD), as well as IR and UV–vis absorption spectroscopies.<sup>12</sup> Powder XRD patterns showed the products to be a mixture of the alkaline-earth fluoride and a second series of peaks later determined by single-crystal XRD to be the alkaline-earth borate fluoride. We note that the patterns (Figure S1 in the Supporting Information, SI) are qualitatively identical, with the peaks of  $Ba_3B_6O_{11}F_2$  shifted to lower angles to account for its larger cell parameters. Targeted syntheses are underway to increase the yield of the borate fluoride compounds and improve upon the 0.4 mm<sup>3</sup> crystal size observed in these initial reactions. Transmission in the UV region is shown in Figure S2 in the SI. The title compounds maintain their UV transparency until an onset of absorption just below 250 nm. The crystals are 50% transparent at about 230 nm, with the transparency falling to 10% at 200 nm, the measurement limit of the instrument used.

The crystallographic parameters from single-crystal structure refinements of the title compounds are summarized in Table 1. The compounds are isostructural and crystallize in the monoclinic space group  $P2_1$ . The acentric space group was confirmed by a qualitative Kurtz experiment.<sup>13</sup> Furthermore,

Received: October 28, 2011

Published: March 12, 2012

**Table 1. Crystallographic Data for Sr<sub>3</sub>B<sub>6</sub>O<sub>11</sub>F<sub>2</sub> and Ba<sub>3</sub>B<sub>6</sub>O<sub>11</sub>F<sub>2</sub>**

empirical formula	Sr <sub>3</sub> B <sub>6</sub> O <sub>11</sub> F <sub>2</sub>	Ba <sub>3</sub> B <sub>6</sub> O <sub>11</sub> F <sub>2</sub>
space group	<i>P</i> 2 <sub>1</sub> (No. 4)	<i>P</i> 2 <sub>1</sub> (No. 4)
<i>a</i> , Å	6.4093(13)	6.5572(13)
<i>b</i> , Å	8.2898(17)	8.5107(17)
<i>c</i> , Å	9.3656(19)	9.6726(19)
β, deg	101.51(3)	101.21(3)
<i>V</i> , Å <sup>3</sup>	487.61(17)	529.49(19)
<i>Z</i>	2	2
<i>fw</i>	541.72	690.88
density (calcd), Mg/m <sup>3</sup>	3.690	4.333
abs coeff, mm <sup>-1</sup>	16.448	11.124
2θ range, deg	3.24–26.33	2.15–25.05
reflns coll'd ( <i>R</i> <sub>int</sub> )	4654 (0.0290)	4359 (0.0598)
indep reflns	1923	1751
obs reflns [ <i>I</i> > 2σ( <i>I</i> )]	1817	1708
final <i>R</i> indices (obsd data) <sup>a</sup>	<i>R</i> 1 = 0.0230, <i>wR</i> 2 = 0.0483	<i>R</i> 1 = 0.0398, <i>wR</i> 2 = 0.0954
<i>R</i> indices (all data)	<i>R</i> 1 = 0.0251, <i>wR</i> 2 = 0.0492	<i>R</i> 1 = 0.0403, <i>wR</i> 2 = 0.0962
GOF ( <i>F</i> <sup>2</sup> )	0.972	1.073
Flack parameter	−0.007(9)	−0.01(4)
largest diff peak, e/Å <sup>3</sup>	0.908	3.10
largest diff hole, e/Å <sup>3</sup>	−0.663	−1.98

$$^a R1 = [\sum ||F_o| - |F_c||] / \sum |F_o|; wR2 = \{[\sum w[(F_o)^2 - (F_c)^2]^2]\}^{1/2}.$$

the observed Flack parameters of −0.007 and −0.01 are consistent with the correct absolute structures for both compounds. The structures are based on a borate fundamental building block (FBB) comprised of four tetrahedrally coordinated and two three-coordinated boron atoms, as shown in Figure 1. The four tetrahedral boron atoms form a

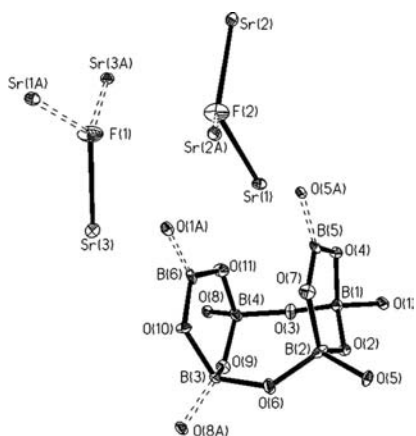


**Figure 1.** Extended asymmetric unit of Sr<sub>3</sub>B<sub>6</sub>O<sub>11</sub>F<sub>2</sub> shown as 50% probability ellipsoids. Dashed bonds to symmetry-related atoms are included to show the local environments of selected atoms.

central four-membered borate ring, and the triangular boron atoms connect to opposing edges of this central ring through shared oxygen atoms. This forms two additional three-membered rings, which share their tetrahedral borates with the central four-membered ring. The [B<sub>6</sub>O<sub>14</sub>] triple-ring structure is described as <Δ2□>=<4□>=<Δ2□> according to the notation of Hawthorne, Burns, and Grice, who have noted that the <Δ2□> ring seen here is quite often a component of large borate clusters such as this.<sup>14,15</sup> Even so, this particular borate cluster in the title compounds is a rather

unusual configuration for six-membered borate FBBs, with the [Φ]<Δ2□>|<Δ2□>|<Δ2□>| arrangement (where three identical rings share a common oxygen vertex) being far more common among the naturally occurring borate minerals. The <Δ2□>=<4□>=<Δ2□> FBB was not observed at all in Becker's survey of anhydrous borate crystal structures.<sup>16</sup>

The <Δ2□>=<4□>=<Δ2□> cluster is somewhat reminiscent of the borate arrangement in natural fabianite [CaB<sub>3</sub>O<sub>5</sub>(OH)].<sup>17</sup> However, the six-membered borate group in fabianite is completed by inversion symmetry, whereas in the title compounds, this is not the case because the triangular borates exhibit a directed polarity (resembling the ears of a cat). The overall polarity imparted on this structure by the borate triangles is apparent in Figure 2. Alignment of the B5- and B6-

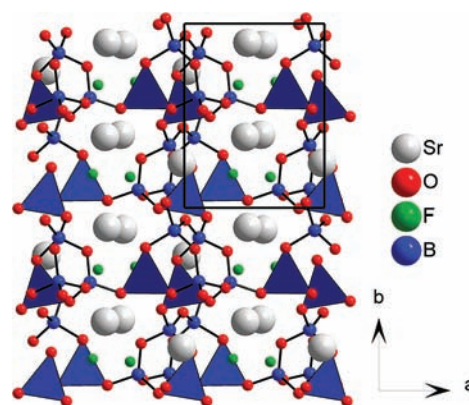


**Figure 2.** Extended structure of Sr<sub>3</sub>B<sub>6</sub>O<sub>11</sub>F<sub>2</sub> viewed along [001]. Triangular borate units are shown as polyhedra to highlight the polarity of the structure.

centered triangles is not exact because they are tilted at about 4.5° and rotated at about 10.3° to one another. The FBBs of the title compounds polymerize much differently from those in fabianite. The [B<sub>6</sub>O<sub>12</sub>(OH)<sub>2</sub>] groups in fabianite connect to one another only through triangular to tetrahedral boron–oxygen bridges to form an overall sheet structure. The title compounds also connect in this way (B6–O1–B1 and B5–O5–B2) but additionally through B3–O8–B4 connections bridging these tetrahedral borates, forming a framework structure. In fabianite, this additional connection is not made because the equivalent oxygen atom in the FBB is, in fact, the hydroxyl group of that structure. The observed B–O bond distances (Table S1 in the SI) in the title compounds are similar to the average values reported in the literature, with slight elongation noted in some tetrahedral B–O bond distances when the shared oxygen atom is bridged to a triangular boron center.<sup>15</sup>

The structure of Sr<sub>3</sub>B<sub>6</sub>O<sub>11</sub>F<sub>2</sub> and Ba<sub>3</sub>B<sub>6</sub>O<sub>11</sub>F<sub>2</sub> also differs significantly from those of the formulaically similar hydrated borates Sr<sub>3</sub>B<sub>6</sub>O<sub>11</sub>(OH)<sub>2</sub> and Ba<sub>3</sub>B<sub>6</sub>O<sub>11</sub>(OH)<sub>2</sub>, which have FBBs also consisting of two triangular and four tetrahedral boron atoms but in a <3□><Δ2□>Δ arrangement (see the corresponding paper in this journal). The hydroxyl groups in those structures are components of the borate FBB, so structural differences arise in that there is not simply a direct structural substitution of F<sup>−</sup> for OH<sup>−</sup> in the borate fluorides. Here, the fluorine atoms of the title compounds are instead bound only to three AE metal atoms rather than serving as part of the borate network (resulting in a [B<sub>6</sub>O<sub>11</sub>] framework for the title compounds compared to a protonated [B<sub>6</sub>O<sub>13</sub>] framework

in the hydrated borates). The fluorine atoms were distinguished by bond-valence analyses, and as expected, the observed Sr–F and Ba–F bond distances (see Table S2 in the SI for Bond Distances and Bond Valences) are noticeably shorter than most of the Sr–O and Ba–O bond distances. If these atoms were instead hydroxyl groups, one would expect the observed bond distances to be elongated because of a reduced electrostatic attraction toward the AE metals. The IR spectrum (Figure S3 in the SI) is consistent with the assignment of the fluorine atoms, showing no bands in the 3000–3500 cm<sup>-1</sup> range diagnostic for OH<sup>-</sup>. Bands corresponding to the stretching vibrations of the borate groups are present at about 1400 and 960 cm<sup>-1</sup>.

All three unique AE metal atoms in each of the title compounds are coordinated by both oxygen and fluorine atoms. Bond distances range from 2.490(6) to 3.236(3) Å for Sr–O, from 2.453(3) to 2.538(3) Å for Sr–F, from 2.698(5) to 3.314(6) Å for Ba–O, and from 2.523(6) to 2.583(6) Å for Ba–F bonds. The AE metal polyhedra form their own network, which fills the gaps in the borate framework. Alkaline-earth metal fluoride bonds are a key aspect of this network because each AE metal has two bonds to fluorine atoms (with AE1 bonding to F1 and F2 atoms, AE2 bonding to two F2 atoms, and AE3 bonding to two F1 atoms). Thus, each unique fluorine atom serves as a common vertex for three AE metal atoms. The fluorine atoms are generally opposite to one another on all AE metal polyhedra, with F–AE–F angles ranging from 153.0(2) to 155.0(3)°. The AE metal polyhedra connect to one another by both edge and corner sharing, and fluorine atoms are involved in both types of connectivity.

In this paper, we report the first of a series of NCS metal borate fluoride crystals grown by the hydrothermal method. The title compounds Sr<sub>3</sub>B<sub>6</sub>O<sub>11</sub>F<sub>2</sub> and Ba<sub>3</sub>B<sub>6</sub>O<sub>11</sub>F<sub>2</sub> in this paper have formulas similar to those of the compounds Sr<sub>3</sub>B<sub>6</sub>O<sub>11</sub>(OH)<sub>2</sub> and Ba<sub>3</sub>B<sub>6</sub>O<sub>11</sub>(OH)<sub>2</sub> described in the corresponding paper, but their structures are very different. The chemical properties of the title compounds make them very promising for deep-UV NLO applications because they have wide band gaps and are thermally stable. Further examination of their optical properties is underway. We feel that the introduction of fluoride in the growth process provides a simple entry to a wide variety of promising new NCS borates.

## ■ ASSOCIATED CONTENT

### ■ Supporting Information

Figures of XRD patterns, UV absorption, and IR absorption, tables of bond distances, bond angles, and bond valences, and crystallographic information files in CIF format. This material is available free of charge via the Internet at <http://pubs.acs.org>.

## ■ AUTHOR INFORMATION

### ■ Corresponding Author

\*E-mail: [kjoseph@clemsun.edu](mailto:kjoseph@clemsun.edu).

### ■ Notes

The authors declare no competing financial interest.

## ■ ACKNOWLEDGMENTS

The authors are grateful for financial support of this project provided by the National Science Foundation (Grant DMR-0907395).

## ■ REFERENCES

(1) Keszler, D. A. *Curr. Opin. Solid State Mater. Sci.* **1996**, *1*, 204.

- (2) Chen, C.; Lin, Z.; Wang, Z. *Appl. Phys. B: Las. Opt.* **2005**, *80*, 1.  
(3) Sasaki, T.; Mori, Y.; Yoshimura, M.; Yap, Y. K.; Kamimura, T. *Mater. Sci. Eng.* **2000**, *30*, 1.  
(4) Becker, P. *Adv. Mater.* **1998**, *10*, 979.  
(5) McMillen, C. D.; Kolis, J. W. *J. Cryst. Growth* **2008**, *310*, 2033.  
(6) Kolis, J. W.; McMillen, C. D.; Franco, T. *Mater. Res. Soc. Symp. Proc.* **2005**, *848*, 3.  
(7) McMillen, C. D.; Giesber, H. G.; Kolis, J. W. *J. Cryst. Growth* **2008**, *310*, 299.  
(8) McMillen, C. D.; Kolis, J. W. *Inorg. Chem.* **2011**, *50*, 6809.  
(9) McMillen, C.; Heyward, C.; Giesber, H.; Kolis, J. *J. Solid State Chem.* **2011**, *184*, 2966.  
(10) Wu, B.; Tang, D.; Ye, N.; Chen, C. *Opt. Mater.* **1996**, *5*, 105.  
(11) Hu, Z.-G.; Yoshimura, M.; Mori, Y.; Sasaki, T. *J. Cryst. Growth* **2004**, *260*, 287.  
(12) Powder XRD patterns were collected from 5 to 65° in 2θ at 1°/min using a Rigaku Ultima IV diffractometer with Cu Kα radiation (λ = 1.5418 Å). Single-crystal XRD was performed using a Rigaku AFC8S diffractometer with Mo Kα (λ = 0.71073 Å) radiation and a Mercury CCD detector. Clear, colorless crystals approximately 0.2 mm<sup>3</sup> in size were selected for single-crystal XRD. A series of 12 screening images were first collected to determine preliminary unit-cell parameter data and identify candidate crystals for the collection of full data sets. Data were collected and processed using the *CrystalClear* software package, and corrections were made for absorption and Lorentz and polarization effects (Molecular Structure Corporation & Rigaku. *CrystalClear, Version 1.3*; Rigaku Corp.: Tokyo, Japan, 2000; MSC, The Woodlands, TX, 2000). The structures were solved by direct methods and refined by full-matrix least squares based on F<sup>2</sup> using the *SHELXTL* software package (Sheldrick, G. M. *Acta Crystallogr.* **2008**, *A64*, 112–122). Consecutive refinements resulted in final R1 values of 0.0230 and 0.0398 for the strontium and barium analogues, respectively. Powder patterns simulated from the single-crystal determinations were in good agreement with the experimentally collected patterns. Further characterization was also performed by IR absorption spectroscopy (Nicolet Magna 550 FTIR from 500 to 3500 cm<sup>-1</sup>) and UV–vis absorption spectroscopy (Perkin Elmer Lambda 900 UV–vis–near-IR spectrometer from 200 to 800 nm).  
(13) Kurtz, S. K.; Perry, T. T. *J. Appl. Phys.* **1968**, *39*, 3798.  
(14) Burns, P. C.; Grice, J. D.; Hawthorne, F. C. *Can. Mineral.* **1995**, *33*, 1131.  
(15) Hawthorne, F. C.; Burns, P. C.; Grice, J. D. *Boron: Mineralogy, Petrology and Geochemistry*; Reviews in Mineralogy; Grew, E. S., Anovitz, L. M., Eds.; Mineralogical Society of America: Washington, DC, 2002; Vol. 33, pp 41–116.  
(16) Becker, P. Z. *Kristallogr.* **2001**, *216*, 523.  
(17) Konnert, J. A.; Clark, J. R.; Christ, C. L. *Z. Kristallogr.* **1970**, *132*, 241.